Mizutani T, Kondo T, Darmanin S, Tsuda M, Tanaka S, Tobiume M, Asaka M, Ohba Y.	A novel FRET-based biosensor for the measurement of BCR-ABL activity and its response to drugs in living cells.	Clin Cancer Res	16 (15)	3964-3975	2010
Yuuki S, Komatsu Y, Fuse N, Kato T, Miyagishima T, Kudo M, Watanabe M, Tateyama M, Kunieda Y, Wakahama O, Sakata Y, Asaka M.	Modified-irinotecan/fluorouracil/levoleucovorin therapy as ambulatory treatment for metastatic colorectal cancer: results of phase I and II studies.	Clin Drug Investig	30 (4)	243-249	2010
武田 宏司、武藤 修一、大西 俊介、浅香 正博	機能性ディスペプシアおよび食欲不振に対する漢方治療	日本消化器病学会雑誌	107 (10)	1586-1591	2010
Suzuki H, Hashimoto H, Kawasaki M, Watanabe M, Otsubo H, Ishikura T, Fujihara H, Ohnishi H, Onuma E, Yamada-Okabe H, Takuwa Y, Ogata E, Nakamura T, Ueta Y.	Similar changes of hypothalamic feeding-regulating peptides mRNAs and plasma leptin levels in PTHrP-, LIF-secreting tumors-induced cachectic rats and adjuvant arthritic rats.	Int J Cancer	128 (9)	2215-2223	2011
Yokoyama T, Ohbuchi T, Saito T, Fujihara H, Minami K, Nagatomo T, Uezono Y, Ueta Y.	Allyl isothiocyanates and cinnamaldehyde potentiate miniature excitatory postsynaptic inputsin the sipraoptic nucleus in rats.	Eur J Pharmacol	655 (1-3)	31-37	2011
Yu D, Nagamura Y, Shimazu S, Naito J, Kaji H, Wada S, Honda M, Xu L, Tsukada T.	Caspase 8 and menin expressions are not correlated in human parathyroid tumors.	Endocr J	57 (9)	825-832	2010
Fujimiya M, Asakawa A, Ataka K, Chen CY, Kato I, Inui A.	Ghrelin, des-acyl ghrelin, and obestatin: regulatory roles on the gastrointestinal motility.	Int J Pept		pii: 305192	2010
Chen CY, Fujimiya M, Laviano A, Chang FY, Lin HC, Lee SD.	Modulation of ingestive behavior and gastrointestinal motility by ghrelin in diabetic animals and humans.	J Chin Med Assoc	73 (5)	225-229	2010
Atsuchi K, Asakawa A, Ushikai M, Ataka K, Tanaka R, Kato I, Fujimiya M, Inui A.	Centrally administered neuromedin s inhibits feeding behavior and gastroduodenal motility in mice.	Horm Metab Res	42 (8)	535-538	2010
Brevet M, Kojima H, Asakawa A, Atsuchi K, Ushikai M, Ataka K, Inui A, Kimura H, Sevestre H, Fujimiya M.	Chronic foot-shock stress potentiates the influx of bone marrow-derived microglia into hippocampus.	J Neurosci Res	88 (9)	1890-1897	2010

IV. 研究成果の刊行物・別刷

ランチョンセミナー

緩和ケアにおける漢方治療

日本大学医学部附属板橋病院緩和ケア室

木下　優子

産婦人科 漢方研究のあゆみ No.27　別刷

発行：2010 年 4 月 20 日
産婦人科漢方研究会

発行所　株式会社 診断と治療社

ランチョンセミナー

緩和ケアにおける漢方治療

日本大学医学部附属板橋病院緩和ケア室

木下　優子

はじめに

漢方は緩和ケアで重要視されるQOL改善に効果がある．また西洋医学の治療における副作用軽減でも漢方治療は有効である．そこで日本大学医学部附属板橋病院では緩和ケアにおいて漢方を積極的に取り入れており，緩和ケアチームにも平成15年の発足時より，東洋医学科の医師が加わっている．また院内で整備されている症状緩和マニュアルにも漢方の項目がある．今回は緩和ケアでよく使用される医療用エキス製剤について，症状緩和マニュアルにある項目を中心に説明する．

Ⅰ　緩和ケアでの漢方薬の使い方（表1）

漢方を使う場面としては全身倦怠感，免疫力増強，食欲不振等が多く，それに次いで，副作用や随伴症状の軽減(嘔気嘔吐，吃逆など)が多い．

1. 全身倦怠感

・免疫力強化，全身倦怠感の改善の基本処方：十全大補湯エキス3包分3.

・効果：免疫力強化・全身倦怠感の改善・放射線治療，化学療法の副作用軽減など.

漢方でいう「補剤」―身体を補い，体力をつける薬．悪性腫瘍に対してQOLの改善のために最もよく使われる処方である．患者さんが免疫力をつける漢方薬があると聞いたと言ってきた時には大体，十全大補湯であることが多い．顔色が優れず，全身倦怠感，疲労感，貧血を伴うものの諸症状に使う．慢性消耗性疾患に用いる．皮膚の乾燥，盗汗，口腔内乾燥，手足の冷えなどを伴うことがある．熱状はない．印象としてはかさかさ枯れた感じ，または貧血らしい感じ，バランスの悪さを感じるなどがある．十全大補湯は漢方医学的には気血両虚(**表2**)の薬である．気血両虚とは気虚と血虚が並存する状態である．気とは簡単にい

表1　処方からみる使い方の目標

漢方処方	使い方の目標
十全大補湯	全身倦怠感の改善 QOLの向上 放射線治療・化学療法の副作用軽減
補中益気湯	食欲不振改善 全身倦怠感の改善
茯苓飲	嘔気嘔吐 胃酸の逆流 胃の入り口でつかえて入っていかない
六君子湯	嘔気嘔吐 胃もたれ 原因不明の吐き気
半夏瀉心湯	カンプトテシンの下痢
啓脾湯	その他の抗癌剤による下痢 原因不明の下痢
牛車腎気丸	手足のしびれ
大建中湯	麻痺性イレウス オピオイドによる便秘
立効散	口内炎
呉茱萸湯 芍薬甘草湯	吃逆(しゃっくり)
加味逍遙散 女神散	ホルモン剤による更年期様症状
麻黄湯	ビスフォスフォネート製剤の副作用
田七人参	出血源がはっきりしない出血

表2　気虚と血虚の症状

	気虚	血虚
症状	体がだるい 気力が出ない 食欲がない 疲れやすい 不安になる 食後眠くなる 日中眠くなる 風邪をひきやすい 声が小さい，力がない 胃下垂である	髪が細い，髪の毛が抜けやすい 顔色が青白い 皮膚がかさかさする 手が荒れる，あかぎれができる 爪が割れやすい，段差ができる 唇が乾燥する かかとでストッキングが破れる 足がつりやすい 月経不順 集中力が出ない 眠れない 眼精疲労 手足の先がしびれる めまい感がある ささくれができやすい 貧血がある

うと生体を巡るエネルギーのことで，気虚とはこのエネルギーが低下した状態を指す．具体的には疲れやすい，食欲がない，体がだるいなどの症状である．血とは生体を巡っている赤い液体とその働きのことで，血虚とはこれが不足した状態を指す．貧血は血虚だと解釈できる．それ以外にも，皮膚の乾燥，毛髪の抜けやすさ，白髪など悪性疾患に罹患した時の症状の多くが血虚であると考えられる．そこで，気虚と血虚の両方を補う十全大補湯が頻用処方であり，かつ有効である．

食欲不振が強く，十全大補湯が服用できない場合は補中益気湯エキス3包分3とする．

2. 食欲不振

・基本処方：補中益気湯エキス3包分3.

補中益気湯は気虚の処方であり，通常の外来では疲れやすいという時に最もよく使われる処方である．そのことから癌による全身倦怠感にも用いられる．食欲不振，食事を食べていると砂を噛んでいるような味気ない感じがする，食後眠いなど食に関する異常を訴えることが多い．様々な疲労や全身倦怠感の治療に使われる．微熱，手足の倦怠感，言葉や眼に力がない，熱いものを好む，口中に白沫が出る，動悸，などの症状を認めることがある．

胃での症状では主として2つの処方が用いられる．茯苓飲と六君子湯である．入り口の茯苓飲，出口の六君子湯と覚えると覚えやすい．

・胃の入り口でつかえてうまく入っていかない場合：茯苓飲エキス3包分3.

機能的な異常はもちろん，器質的な狭窄があっても有効な場合がある．飲んでしばらくは食べられるというケースが多いので食直前の投与にすることが多い．通過障害を伴う場合が多いので，煎じ薬にするかお湯に溶いて内服させる．茯苓飲は「呑酸」といって胃酸の逆流に対しても有効な処方である．ストレスが強くてのどのつかえ感を伴う場合(漢方では「咽中炙臠(のどに炙った肉がつかえたような感じ)」という)には，茯苓飲合半夏厚朴湯を用いるが，通過障害には茯苓飲のみのほうがよく効く．よりシンプルな処方にしたほうが効果は得やすいのである．

・胃もたれ感が強い・胃の中に物がたまって出て行かない場合：六君子湯エキス3包分3.

最近，機能性ディスペプシア(functional dyspepsia：FD)に有効であることで注目を集めている処方であるが，胃もたれする時の頻用処方である．胃の内容物を送り出す作用があることから，食べるとすぐお腹がいっぱいになってしまうという時に有効．食欲増進効果も期待できる．

3. 嘔気・嘔吐

嘔気嘔吐も食欲不振とほぼ同じ処方を使用する．

・胃酸の逆流がある場合：茯苓飲エキス3包分3.
・胃もたれ感が強い場合：六君子湯エキス3包分3.

漢方薬はエキス剤か煎じ薬であるためにドラッグコンプライアンスが悪く，嘔気嘔吐がある時に

は内服は困難である．しかし，六君子湯は難治性の嘔気嘔吐で著効を示すことがあり，他の薬が無効であるときには選択を検討すべきであると考える．実際，乳癌の50歳代女性でナウゼリン®，プリンペラン®，ノバミン®，セレネース®すべて無効でアタラックス-P®のみやや有効であった症例で六君子湯だけが効果があった．

気分の落ち込みが強い時には鬱状態の時に使われる香蘇散エキスを併用することがある．

化学療法による嘔吐については茯苓飲も使うが，十全大補湯の事前投与が有効であることが多い(次項参照)．

4. 放射線治療・化学療法の副作用軽減

いずれも開始前(できれば2週間以上)より十全大補湯エキス3包分3を投与する．

投与することによって副作用の軽減を図ることができる．それまで抗癌剤を投与するたびに白血球減少のために次のクールに入るのが遅れていた患者が計画通り治療できるようになったり，嘔気嘔吐の回数を減らしたりすることができる．もちろん，全身倦怠感の改善にも有効であるため，抗癌剤で癌は縮小しているものの，投与するたびに全身倦怠感が強く，何もできないといったことを改善し，QOLの向上に寄与することも可能である．

放射線治療や化学療法の副作用は漢方での気血両虚に相当する症状が多い．嘔気嘔吐や食欲不振は気虚にあたる．白血球減少や貧血，脱毛，口内炎，皮膚のやけどなどは血虚にあたる．そのため，十全大補湯の事前投与が有効になる．ここで問題になるのは事前投与ということである．早く始めてもらったほうが効果がある．そこで，漢方は未病を治す(病気と認定される前の症状を治して，病気にならないようにする)といっても，事前投与は意味があるのかという議論がある．しかし，放射線治療や化学療法を行う患者は大きな手術を受けていたり，あるいは手術不能例であることが多い．大きな手術を受けていればそのときの侵襲や出血により気血両虚に陥っている可能性は高い．手術不能例では現病によって全身状態の悪化をみて気血両虚であることが多い．そのため事前投与が推奨されるのである．

胸椎に放射線治療を行っている時の食道の不快感には加味逍遙散エキス3包分3を用いる．これは構成生薬の一つである山梔子の清熱作用が有効であると考えられている．西洋医学ではよくアルロイドGを用いるが，これが飲みにくいという場合には漢方薬も選択できる．また両者を併用することも可能である．

化学療法中の嘔吐には茯苓飲エキスを投与する(3包分3または頓服)．症状に応じて，四君子湯エキスや六君子湯エキスを選択することもある．しかし，治療中は嘔気が強いため，内服自体が困難なことも多く，十全大補湯の事前投与が第一選択となる．

【化学療法中の下痢】

- カンプトテシンの下痢：半夏瀉心湯エキス3包分3.
- それ以外の場合：啓脾湯エキス3包分3.
- 化学療法時のしびれ：牛車腎気丸エキス3包分3.

特にドセタキセルの副作用によるしびれに有効であるとして知られているのが牛車腎気丸である．しかし，オンコビンなどのしびれにはさほど効かないため，十全大補湯の併用が必要になる．

5. 便秘

- イレウスやモルヒネによる便秘：大建中湯エキス6包分3.

大建中湯は腸管蠕動を亢進させ，腸管の血流改善作用があることで知られており，麻痺性イレウスの頻用処方である．腸管蠕動を改善することからオピオイドによる便秘にも有効である．大建中湯の優れているところは下痢の時も内服継続できる点である．下痢と便秘を繰り返す患者は多く，下剤の調節は苦労することが多い．大建中湯は腸管蠕動を亢進させる作用が注目されているが，本来は蠕動を調節する作用をもつ処方であり，下痢の時には抑える効果を示すことがある．

6. 口内炎

立効散エキス1包をお湯に溶かして，口の中に含ませる．1日数回．

ただし，化学療法・放射線治療中の口内炎は血虚による影響が大きいため，十全大補湯の事前投与のほうが有効である．

7. 吃逆

呉茱萸湯エキスをお湯に溶かして内服させる．1日目：9包分3，2日目以降：6包分3で投与．または芍薬甘草湯を吃逆時，頓服．いずれも無効な場合は柿蒂(してい)の使用を検討する．

呉茱萸湯は頭痛の処方として知られているが，吃逆にも有効である．しかし，悪性疾患に伴う吃逆の場合には通常より多く内服させる必要がある．また冷えを伴っている場合が多いため，お湯に溶かして内服させることが重要である．エキスをそのまま水で内服させると効かないことがある．

芍薬甘草湯は下肢の痙攣に使う処方として知られているが，筋肉の緊張をとる作用があり，頭痛や吃逆にも用いられる．ただし，甘草を多く含むため偽アルドステロン症のリスクがあり，長期の連用には注意が必要である．そのために頓服とすることが望ましい．

柿蒂は柿のへたで民間療法で吃逆に用いられるものである．そのため医療用のエキス製剤にはないが，市販の漢方薬として存在する．

8. ホルモン剤による副作用

よくみられる症状が更年期様症状であるため，更年期症候群の頻用処方である加味逍遙散3包分3が用いられることが多い．また，のぼせが強い時は女神散エキス3包分3を用いる．この場合もベースに十全大補湯を内服させることは多く，十全大補湯がないと取れないのぼせも存在する．それ以外に，むくみには当帰芍薬散・五苓散，冷えには当帰四逆加呉茱萸生姜湯，下腹部の不快感には温経湯などを使い分ける．

9. ビスホスホネート製剤(ゾメタ®)の副作用による痛み・発熱

ゾメタ®投与時より麻黄湯エキス3包分3を3日間内服．

発熱や激しい骨痛が風邪やインフルエンザで麻黄湯を使用する目標に近いことから使用を始めたところ，有効であった．特に外来で治療していて働いている人では，ゾメタ®投与後の社会復帰を早める効果があり，QOL向上につながると考えられた．

10. 下血などの消化管出血

田七人参(粉末)を3g分3．

田七人参は医療用のエキス製剤ではないが市販されており，滅菌のものも存在するので使用しやすい．下血に限らず出血源のはっきりしない出血では有効である．

おわりに

漢方薬は緩和ケアの様々な場面で応用できる．また患者のなかには緩和ケアというとまだまだ否定的なイメージをもつ患者が強く，末期治療だと考えるものも多い．漢方治療は患者の不快な症状の軽減だけでなくQOLも向上させることから，緩和ケアのイメージアップにもつながる可能性があると考えられる．同時に，西洋医学的治療の副作用軽減も可能であることから，治療の継続にも有効である．漢方は緩和ケアにおいて重要なツールであると考えられる．

J Pharmacol Sci 112, 424 – 431 (2010)

Journal of Pharmacological Sciences

Full Paper

Analysis of the Effects of Anesthetics and Ethanol on μ-Opioid Receptor

Kouichiro Minami[1,3,*], Yuka Sudo[2,3], Seiji Shiraishi[3], Masanori Seo[1], and Yasuhito Uezono[3]

[1]*Department of Anesthesiology and Critical Care Medicine, Jichi Medical University, Tochigi 329-0483, Japan*
[2]*Department of Molecular and Cellular Biology, Nagasaki University School of Biomedical Sciences, Nagasaki 852-8523, Japan*
[3]*Cancer Pathophysiology Division, National Cancer Center Research Institute, Tokyo 104-0045, Japan*

Received January 6, 2010; Accepted February 15, 2010

Abstract. G protein–coupled receptors, in particular, Ca^{2+}-mobilizing G_q-coupled receptors have been reported to be targets for anesthetics. Opioids are commonly used analgesics in clinical practice, but the effects of anesthetics on the opioid μ-receptors (μOR) have not been systematically examined. We report here an electrophysiological assay to analyze the effects of anesthetics and ethanol on the functions of μOR in *Xenopus* oocytes expressing a μOR fused to chimeric Gα protein G_{qi5} (μOR-G_{qi5}). Using this system, the effects of halothane, ketamine, propofol, and ethanol on the μOR functions were analyzed. In oocytes expressing μOR-G_{qi5}, the μOR agonist DAMGO ([D-Ala^2,*N*-MePhe^4,Gly-ol]-enkephalin) elicited Ca^{2+}-activated Cl^- currents in a concentration-dependent manner (EC_{50} = 0.24 μM). Ketamine, propofol, halothane, and ethanol themselves did not elicit any currents in oocytes expressing μOR-G_{qi5}, whereas ketamine and ethanol inhibited the DAMGO-induced Cl^- currents at clinically equivalent concentrations. Propofol and halothane inhibited the DAMGO-induced currents only at higher concentrations. These findings suggest that ketamine and ethanol may inhibit μOR functions in clinical practice. We propose that the electrophysiological assay in *Xenopus* oocytes expressing μOR-G_{qi5} would be useful for analyzing the effects of anesthetics and analgesics on opioid receptor function.

Keywords: μ-opioid receptor, $G_{i/o}$-coupled receptor, ketamine, ethanol, *Xenopus* oocyte

Introduction

Opioids are commonly used analgesics in clinical practice, but the role of opioid receptor (OR) in anesthetic action has still been unclear. It has been reported that the OR antagonist naloxone does not affect the anesthetic potency of volatile anesthetics halothane in animals (1, 2). On the other hand, Sarton et al. reported that S(+) ketamine interacts with the μ-opioid system at supraspinal sites (3). In order to clarify the role of ORs in anesthetic action, it would be necessary to study the direct effects on OR function.

Several lines of studies have been reported that metabotropic G protein–coupled receptors (GPCRs) are now recognized as targets for anesthetics and analgesics (4). We and others have previously reported that functions of G_q protein–coupled receptors, including muscarinic type1 receptors (M_1R) (5), metabotropic type 5 glutamate receptors (mGluR5) (6), 5-hydroxytryptamine (5HT) type 2A receptors (7), and substance P receptors (8), are inhibited by anesthetics and analgesics. The ORs belong to the GPCR family and three types of ORs, μ, δ, and κ, have been identified by molecular cloning (9). Within three subtypes of these receptors, μORs are the major receptor to mediate the analgesic effects of opioids (9). On the basis of second messenger signaling, μOR couple to $G\alpha_{i/o}$ protein to cause inhibition of adenylate cyclase, inhibition of voltage-dependent Ca^{2+} channels, or activation of G protein–coupled inwardly rectifying K^+ channels (GIRKs) (9). Functions of G_q-coupled receptors have been reported to be modified by some anesthetics and analgesics (4, 10); as far as the functions of $G_{i/o}$-coupled receptors including μOR are concerned, much less is known about the direct effects of anesthetics and analgesics.

The *Xenopus* oocyte expression system has widely

*Corresponding author. kminami@med.uoeh-u.ac.jp
Published online in J-STAGE on April 2, 2010 (in advance)
doi: 10.1254/jphs.10003FP

been employed to study functions of a number of GPCRs (4, 10). In the case of G_q-coupled receptors, stimulation of the receptors result in activation of Ca^{2+}-activated Cl^- currents in *Xenopus* oocytes by G_q-mediated activation of phospholipase C (PLC) and subsequent formation of IP_3 and diacylglycerol (4, 11). The IP_3 formed causes release of Ca^{2+} from the endoplasmic reticulum by activation of IP_3 receptors (IP_3R), which in turn, triggers the opening of Ca^{2+}-activated Cl^- channels endogenously expressed in the oocytes (4, 11). However, in the case of $G_{i/o}$-coupled receptors, analysis has been difficult due to lack of appropriate analytical output in oocytes. We have established the assay method for $G_{i/o}$-coupled receptors by using G_{qi5} chimeric G protein to switch the $G_{i/o}$ signal to a G_q signal (12). By using this assay system, we reported that halothane inhibited the function of $G_{i/o}$-coupled muscarinic M_2 receptor (M_2R) in oocytes coexpressing M_2R and G_{qi5} (13). Recently, in order to improve the $G_{i/o}$-coupled–receptor assay system, we made a μOR fused to G_{qi5} (μOR-G_{qi5}) and expressed it in *Xenopus* oocytes (13).

By using this assay system, we examined the effects of halothane, ketamine, propofol, and ethanol on the function of μOR.

Materials and Methods

Materials

Adult *Xenopus laevis* female frogs were purchased from Kato Kagaku (Tokyo); halothane, from Dinabot Laboratories (Osaka), and the Ultracomp *E. coli* Transformation Kit, from Invitrogen (San Diego, CA, USA). Purification of cDNAs was performed with a Qiagen purification kit (Qiagen, Chatworth, CA, USA). Gentamicin, sodium pyruvate, [D-Ala^2,*N*-MePhe^4,Gly-ol]-enkephalin (DAMGO), and propofol were purchased from Tokyo Kagaku (Tokyo), and ketamine was purchased from Sigma (St. Louis, MO, USA). Other chemicals are analytical grade and were from Nacalai Tesque (Kyoto). The rat μOR was provided by Dr. N. Dascal (Tel Aviv University, Ramat Aviv, Israel). The chimeric $G\alpha_{qi5}$ was a kind gift from Dr. B.R. Conklin (The University of California, San Francisco, CA, USA). Each of the cRNAs was prepared by using an mCAP mRNA Capping Kit and transcribed with a T7 RNA Polymerase in vitro Transcription Kit (Stratagene, La Jolla, CA, USA).

Preperartion of chimeric μOR-Gqi5

The tandem cDNAs of chimeric μOR-G_{qi5} was created by ligating the receptor cDNA sequences into the NheI site of G_{qi5} cDNAs. The sequences of all PCR products were confirmed by sequencing with ABI3100 (Applied BioSystems, Tokyo). All cDNAs for the synthesis of cRNAs were subcloned into the pGEMHJ vector, which provides the 5′- and 3′-untranslated region of the *Xenopus* β-globin RNA (14), ensuring a high level of protein expression in the oocytes. Each of the cRNAs was synthesized using the mCAP mRNA Capping Kit, with the T7 RNA polymerase in vitro Transcription Kit (Ambion, Austin, TX, USA) from the respective linearized cDNAs.

Recording and data analyses

Isolation and microinjection of *Xenopus* oocytes were performed as previously described (12, 13). *Xenopus* oocytes were injected with appropriate amounts of cRNAs (50 ng, μOR-G_{qi5}) and incubated with ND 96 medium composed of 96 mM NaCl, 2 mM KCl, 1.8 mM $CaCl_2$, 1 mM $MgCl_2$, 5 mM HEPES (pH 7.4, adjusted with NaOH), supplemented with 2.5 mM sodium pyruvate and 50 μg/ml gentamicin for 3 – 7 days until recording. Oocytes were placed in a 100-ml recording chamber and perfused with MBS (modified Barth's saline) composed of 88 mM NaCl, 1 mM KCl, 2.4 mM $NaHCO_3$, 10 mM HEPES, 0.82 mM $MgSO_4$, 0.33 mM $Ca(NO_3)_2$, and 0.91 mM $CaCl_2$, (pH 7.4 adjusted with NaOH) at a rate of 1.8 ml/min at room temperature. Recording and clamping electrodes (1 – 2 MΩ) were pulled from 1.2-mm outside diameter capillary tubing and filled with 3 M KCl. A recording electrode was imbedded in the animal's pole of oocytes, and once the resting membrane potential stabilized, a clamping electrode was inserted and the resting membrane potential was allowed to restabilize. A Warner OC 725-B oocyte clamp (Hampden, CT, USA) was used to voltage-clamp each oocyte at −70 mV. We analyzed the peak component of the transient inward currents induced by receptor agonists because this component is dependent on the concentrations of the receptor agonist applied and is quite reproducible, as described by Minami et al. (15). Anesthetics (halothane, ketamine, propofol) and ethanol were applied for 2 min before and during the application of test compounds to allow complete equilibration in the bath. The solutions of halothane were freshly prepared immediately before use. We calculated the final concentration of halothane in the recording chamber as reported previously (16), and accordingly, the concentrations of halothane represent the bath concentrations.

Statistical analyses

Results are expressed as percentages of control responses. The control responses were measured before and after each drug application, to take into account possible shifts in the control currents as recording proceeded. The "n" values refer to the number of oocytes studied. Each experiment was carried out with oocytes from at

least two different frogs. Statistical analyses were performed using a one-way ANOVA (analysis of variance) and the Dunnet correction. Curve fitting and estimation of EC_{50} values for the concentration–response curves were performed using Graphpad Inplot Software (San Diego, CA, USA).

Results

DAMGO-induced Ca^{2+}-activated Cl^- currents in Xenopus oocytes expressing μOR-G_{qi5}

We first determined the effects of the μOR agonist DAMGO on the Ca^{2+}-activated Cl^- currents in *Xenopus* oocytes expressing μOR-G_{qi5}. As shown in Fig. 1A, DAMGO at 0.1 μM elicited a robust Ca^{2+}-activated Cl^- current. There were no Cl^--currents in oocytes expressing μOR not fused to G_{qi5} even at 10 μM DAMGO (data not shown), as reported previously (13). The EC_{50} of the DAMGO-induced Cl^- currents was 0.24 ± 0.01 μM (Fig. 1B).

Analysis of ketamine and propofol on DAMGO-induced Ca^{2+}-activated Cl^- currents in Xenopus oocytes expressing μOR-G_{qi5}

By using this assay, we examined the effects of the intravenous anesthetic ketamine on the μOR function in *Xenopus* oocytes expressing μOR-G_{qi5}. Ketamine by itself did not elicit any currents in oocytes expressing μOR-G_{qi5} but significantly inhibited DAMGO-induced Ca^{2+}-activated Cl^- currents in a concentration-dependent manner (Fig. 2A). Ketamine at 0.1, 1, and 10 μM inhibited the

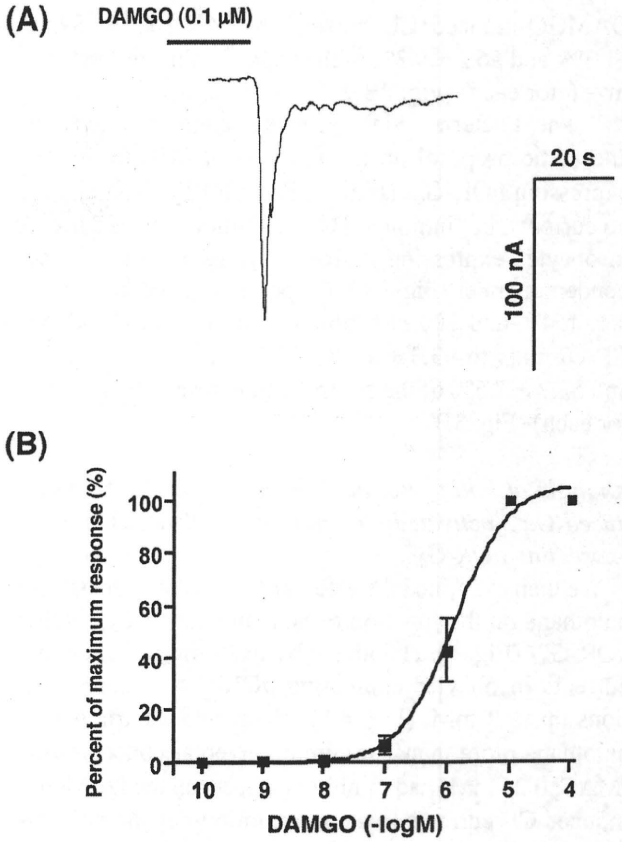

Fig. 1. Electrophysiological μOR assay induced by the μOR agonist DAMGO in *Xenopus* oocytes expressing μOR-G_{qi5}. A: Typical tracing of DAMGO (0.1 μM)–induced Ca^{2+}-activaed Cl^- current in an oocyte expressing μOR-G_{qi5}. B: Concentration–response curves of DAMGO-induced Ca^{2+}-activated Cl^- currents in oocytes. Oocytes were voltage-clamped at −70 mV and DAMGO was applied for 20 s.

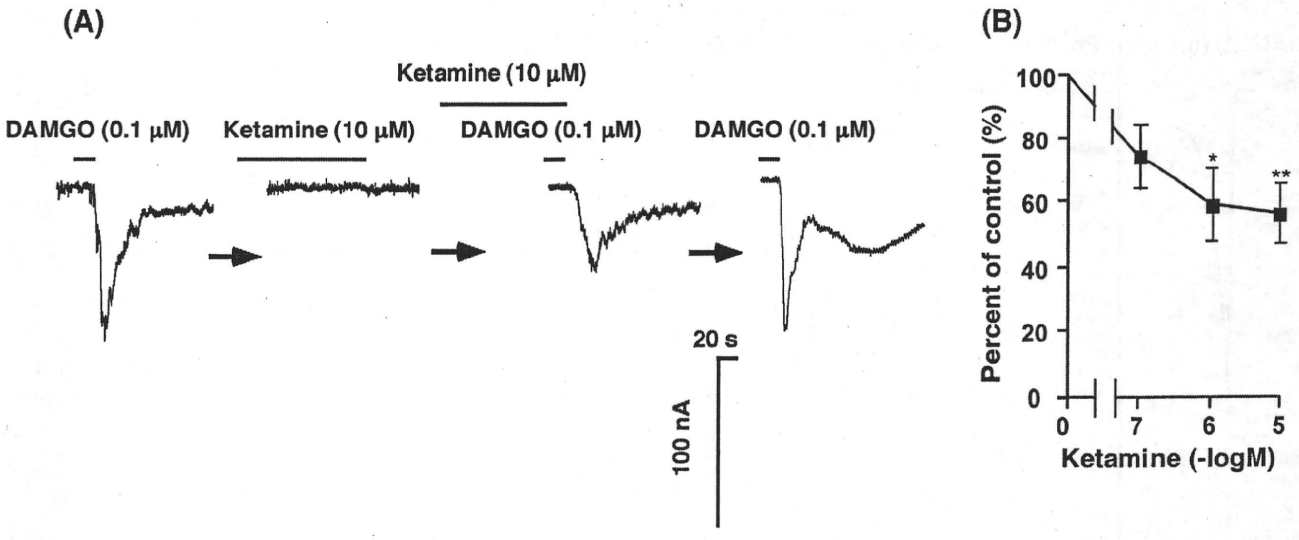

Fig. 2. Effects of ketamine on the basal and DAMGO-induced Ca^{2+}-activated Cl^- currents in oocytes expressing μOR-G_{qi5}. A: Typical tracings of the effect of 10 μM ketamine on the Cl^- current evoked by 0.1 μM DAMGO in an oocyte expressing μOR-G_{qi5}. B: Concentration–response curve for the inhibitory effects of ketamine on DAMGO (0.1 μM)–induced Cl^- currents in oocytes expressing μOR-G_{qi5}. $^*P < 0.05$ and $^{**}P < 0.01$ vs. control.

DAMGO-induced Cl^- currents to 74 ± 10.3%, 59.1 ± 11.3%, and 56.2 ± 9.3% of the control value, respectively (n = 6 for each) (Fig. 2B).

We next determined the effects of another intravenous anesthetic propofol on the function of μOR in oocytes expressing μOR-G_{qi5} (Fig. 3). Propofol by itself elicited no currents, but inhibited DAMGO-induced Cl^- currents in oocytes expressing μOR-G_{qi5} in a concentration-dependent manner (Fig. 3A). Propofol at concentrations of 0.1, 1, 10, and 100 μM inhibited the DAMGO-induced Cl^- currents to 93.3 ± 3.7%, 73.5 ± 7.9%, 72.8 ± 5.7%, and 53.7 ± 7.5% of the control value, respectively (n = 6 for each) (Fig. 3B).

Analysis of halothane and ethanol on the DAMGO-induced Ca^{2+}-activated Cl^- currents in Xenopus oocytes expressing μOR-G_{qi5}

We then examined the effects of the volatile anesthetic halothane on the function of μOR in oocytes expressing μOR-G_{qi5} (Fig. 4). Halothane by itself did not elicit any currents in oocytes expressing μOR-G_{qi5} at concentrations up to 2 mM, (Fig. 4A). Higher concentrations of halothane more than 1 minimum alveolar concentration (MAC, 0.25 mM) had inhibitory effects on the DAMGO-induced Cl^- currents in a concentration-dependent manner; 1MAC concentration of halothane did not suppress DAMGO-induced Cl^- currents. Halothane at concentrations of 0.25, 0.5, 1, and 2 mM inhibited the current to 75.1 ± 12.4%, 57.8 ± 10.3%, 54.7 ± 10.3%, and 48.6 ± 9.4% of the control value, respectively (n = 6 for each) (Fig. 4B).

We finally examined the effects of ethanol on the function of μOR in oocytes expressing μOR-G_{qi5} (Fig. 5). Ethanol by itself had no effects in oocytes expressing μOR-G_{qi5}, but it significantly inhibited DAMGO-induced Cl^- currents in a concentration-dependent manner (Fig. 5B). Ethanol at concentrations of 25, 50, 100, and 200 mM inhibited the currents to 53.1 ± 10.1%, 47 ± 13.3%, 43.3 ± 9.6%, and 35 ± 5.3% of the control value, respectively (n = 6 for each) (Fig. 5B).

Discussion

We previously proposed an electrophysiological assay of the $G_{i/o}$-coupled receptors in *Xenopus* oocytes expressing the receptors and chimeric G protein G_{qi5} (12, 13). By using this system, we examined the effects of several anesthetics and ethanol on the μOR function in oocytes expressing fused μOR-G_{qi5}.

In general, $G_{i/o}$-coupled receptors such as μOR are known to inhibit adenylate cyclase to decrease cAMP levels in the cells (9). Numerous reports have shown that ketamine, halothane, and ethanol increase basal cAMP levels in a variety of the cells, possibly by direct activation of adenylate cyclases (17 – 20); thus it might be difficult to estimate the effects of anesthetics and ethanol

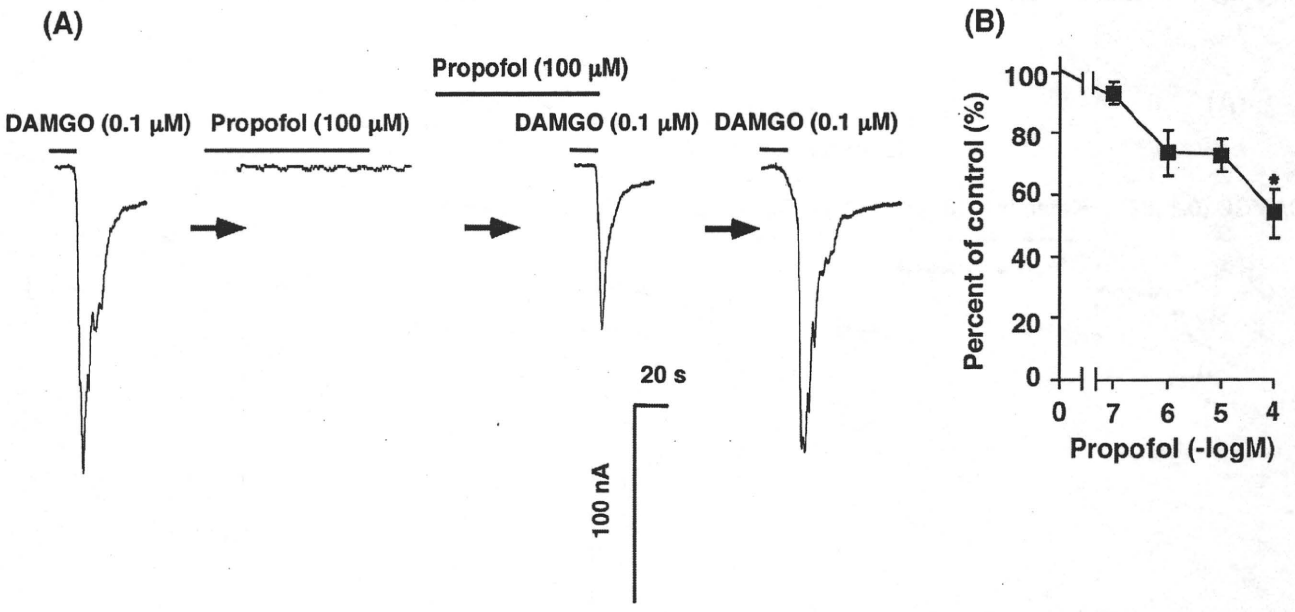

Fig. 3. Effects of propofol on the basal and DAMGO-induced Ca^{2+}-activated Cl^- currents in oocytes expressing μOR-G_{qi5}. A: Typical tracings of the effect of 100 μM propofol on the Cl^- current evoked by 0.1 μM DAMGO in an oocyte expressing μOR-G_{qi5}. B: Concentration–response curve for the inhibitory effects of propofol on DAMGO (0.1 μM)–induced Cl^- currents in oocytes expressing μOR-G_{qi5} *$P < 0.05$ and vs. control.

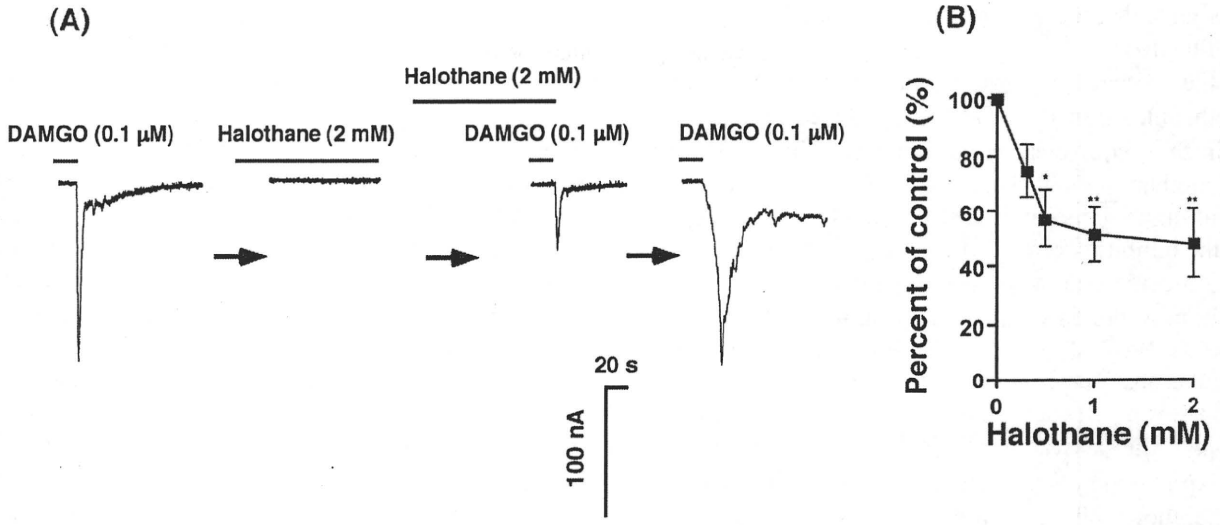

Fig. 4. Effects of halothane on the basal and DAMGO-induced Ca^{2+}-activated Cl^- currents in oocytes expressing μOR-G_{qi5}. A: Typical tracings of the effect of 2 mM halothane on the Cl^- current evoked by 0.1 μM DAMGO in an oocyte expressing μOR-G_{qi5}. B: Concentration–response curve for the inhibitory effects of halothane on DAMGO (0.1 μM)–induced Cl^- currents in oocytes expressing μOR-G_{qi5}. $^*P < 0.05$ and $^{**}P < 0.01$ vs. control.

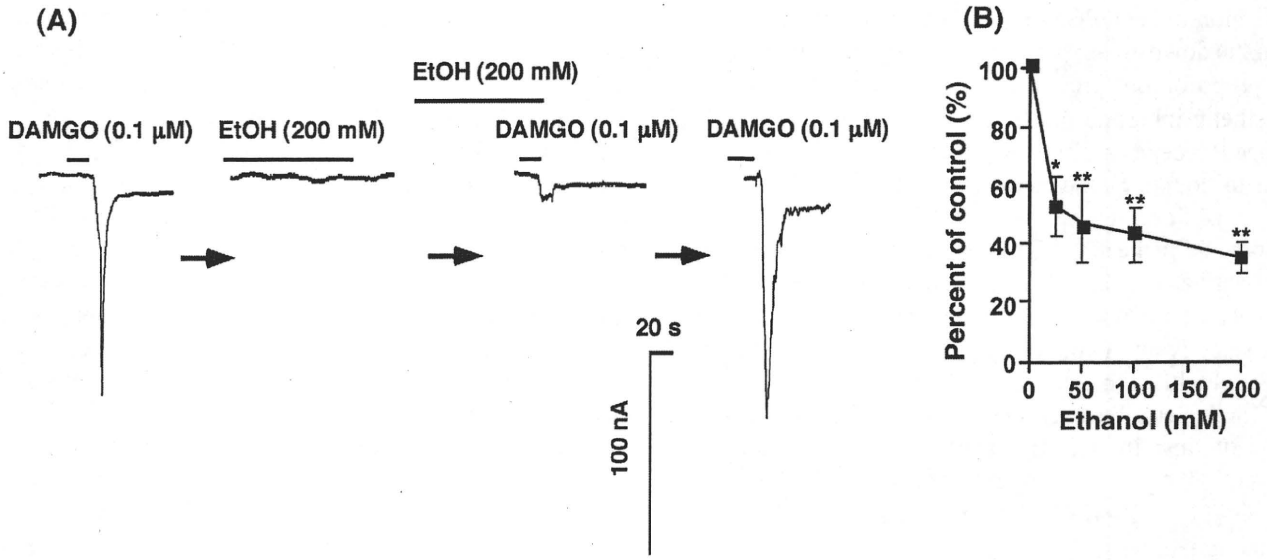

Fig. 5. Effects of ethanol on the basal and DAMGO-induced Ca^{2+}-activated Cl^- currents in oocytes expressing μOR-G_{qi5}. A: Typical tracings of the effect of 200 mM ethanol on the Cl^- current evoked by 0.1 μM DAMGO in an oocyte expressing μOR-G_{qi5}. B: Concentration–response curve for the inhibitory effects of ethanol on DAMGO (0.1 μM)–induced Cl^- currents in oocytes expressing μOR-G_{qi5}. $^*P < 0.05$ and $^{**}P < 0.01$ vs. control.

on the functions of $G_{i/o}$-coupled receptors by using a cAMP inhibition assay. Alternatively we and others have used *Xenopus* oocytes expressing GIRK channels for the analysis of functions of $G_{i/o}$-coupled receptors such as μOR, $GABA_BR$, or cannabinoid CB_1 and CB_2 receptors (13, 21 – 23); GIRKs have been demonstrated to be excellent reporter channels for assay of the activity of $G_{i/o}$-coupled receptors (21). However, recent reports have revealed that GIRKs are possible targets for several anesthetics including halothane and ethanol (24 – 26). In such a situation, it should be taken into consideration that functions of either $G_{i/o}$-coupled receptors, GIRKs, or both could be affected by anesthetics or alcohol if GIRKs are used as reporters (24 – 26). In this study, we thus employed μOR-G_{qi5} in a *Xenopus* oocyte expression assay system. Accordingly, this system makes it possible

to study the direct effects of anesthetics and alcohols on μOR functions.

In the present study, we demonstrated that ketamine and ethanol inhibited the DAMGO-induced Cl^- currents at clinically equivalent concentrations, while propofol and halothane inhibited the DAMGO-induced currents only at higher concentrations. In our experimental system, the inhibitory effects of the anesthetics and ethanol are considered due to specific inhibition of μOR or the inhibition of the downstream steps in the μOR-induced G_{qi5}–PLC–IP_3–IP_3R–Ca^{2+} mobilization pathways. There are numerous reports showing that ketamine, propofol, halothane, and ethanol did not inhibit such downstream pathways after activation of GPCRs in the *Xenopus* oocyte expression system. In the case of ketamine and halothane, they inhibit muscarinic M_1R-mediated Ca^{2+}-activated Cl^- currents in clinically relevant concentrations (5, 27) without affecting angiotensin II receptor (AT_1R)–induced Cl^- currents, although activation of M_1R and AT_1R consequently activate the same G_q–PLC–IP_3–IP_3R–Ca^{2+} mobilization pathways (5, 27). These results suggest that ketamine and halothane affect functions of Ca^{2+}-mobilizing GPCRs possibly by receptor sites rather than the downstream pathway after GPCR activation. As for propofol, our previous study demonstrated that this anesthetic inhibited the functions of M_1R but not substance P receptors, although both receptors were considered to couple to the same Gq-mediated pathways (8, 28). In addition, we demonstrated that propofol (50 μM) did not inhibit the direct G protein activator AlF_4^-–induced Ca^{2+}-activated Cl^- currents in *Xenopus* oocytes (28). In the case of ethanol, we previously reported that ethanol also selectively inhibited the glutamate mGluR5 but not mGluR1, although both receptors couple to Gq to activate Ca^{2+}-activated Cl^- currents in oocytes (6). Taken together, these findings indicate that anesthetics and ethanol employed in the present study may not inhibit the step of G protein–PLC–IP_3–IP_3R–Ca^{2+} mobilization in the μOR signaling pathway.

The EC_{50} value of DAMGO of the μOR-induced Ca^{2+}-activated Cl^--currents through G_{qi5} was 0.24 μM in the present study. In our previous experimental study in *Xenopus* oocytes expressing μOR-G_{qi5} (13), the EC_{50} of DAMGO was approximately 0.1 μM. In *Xenopus* oocytes expressing cloned μOR and GIRKs, the EC_{50} values of DAMGO were 0.1 (13), 0.034 – 0.133 (29), and 0.02 – 0.09 μM (30) determined with the GIRK channel assay. These results suggest that our present EC_{50} value seems not too far from the previously reported EC_{50} values obtained in *Xenopus* oocytes expressing μOR.

We showed that ketamine had an inhibitory effect on DAMGO-induced Cl^- currents in oocytes expressing μOR-G_{qi5} at concentrations more than 1 μM. In clinical situations, the free plasma concentration of ketamine was approximately 10.5 – 60 μM (31, 32). Previous reports showed that higher concentration of ketamine than those in clinical usage (50 – 100 μM) displaced [^{3}H]diprenorphine binding to μORs expressed in Chinese hamster ovary cells (33). In an animal study, S(+)ketamine interacts with the μOR, which contributed to S(+)ketamine-induced respiratory depression and supraspinal antinociception (3). Consistent with these reports, our present results suggest that anesthetic concentrations of ketamine would have direct inhibitory effects on μOR.

The effects of propofol on the μOR functions have not been reported so far. In the present study, only high concentration (100 μM) of propofol (but less than 100 μM) had inhibitory effects on the DAMGO-induced Cl^- currents in oocytes expressing μOR-G_{qi5}. In humans, the peak plasma concentration of propofol after intravenous injection of the anesthetic dosage of 2.5 mg/kg was approximately 23 ± 0.24 μM (34). From our present results, it seems that propofol would have little effect on the μOR functions in its clinically used concentrations.

The direct effects of halothane on the μOR have not been studied. In the present study, clinical concentrations of halothane (0.25 mM) had no effect on basal- and DAMGO-induced Cl^- currents in *Xenopus* oocytes expressing μOR-G_{qi5}, whereas higher concentrations of halothane (0.5 – 2.0 mM) inhibited the DAMGO-induced Cl^- currents. To our knowledge, this is the first report that shows the direct effects of halothane on the function of μOR in the heterologous expression system. Lambert et al. have reported that binding of [^{3}H]DAMGO was unaffected by lower concentrations of halothane, but 5.0% (approximately 5.3 MAC) halothane reduced its affinity (35). From our present and previous reports, higher concentrations of halothane would inhibit the DAMGO-induced currents by reducing the affinity of DAMGO to μOR. Yamakura et al., on the other hand, reported that inhibition by halothane is likely caused by inhibition of GIRK channels, not by μOR (25). Furthermore, it was recently reported that the MACs for halothane are not different between wild-type and μOR–knock-out mice (36). Although further study would be necessary, our present result suggests that halothane would have little effect on μOR in the clinical situation.

Interaction between alcohol and the CNS opioid signaling system is well established in both basic and clinical research (37, 38). However, mechanisms involving direct ethanol interaction on the μOR have not been fully elucidated. We showed that ethanol at a concentration more than 25 mM inhibited DAMGO-induced Cl^- currents in oocytes expressing μOR-G_{qi5}. Several hypotheses of such inhibitory effects have been asserted; Vukojević et al. reported that relevant concentrations of ethanol

(10 – 40 mM) altered μOR mobility and surface density and affect the dynamics of plasma membrane lipids of pheochromocytoma PC12 cells, suggesting that ethanol modified μOR activity by sorting of μOR at the plasma membrane (39). Although further studies will be required, ethanol might inhibit the DAMGO-induced currents by reducing the affinity of DAMGO to the μOR.

In conclusion, we demonstrated that ketamine and ethanol have significant inhibitory effects on the function of μOR at clinically relevant concentrations. On the other hand, halothane and propofol seem not to suppress the μOR functions at least at clinically used concentrations. Further studies will be necessary to clarify the effects of these agents on opioid systems with other assay systems. The electrophysiological method for analysis of the function of μOR fused to the chimeric Gα protein shown in this study could be useful for investigating the effects of analgesics, anesthetics, and alcohol on other $G_{i/o}$-coupled receptors.

Acknowledgments

The authors would like to thank all the members in Cancer Pathophysiology Division in National Cancer Center Research Institute. This work was supported by grants from the Ministry of Education, Culture, Sports, Science, and Technology of Japan (K.M., Y.U.); Smoking foundation (Y.U., Y.S.); Foundation of Daiichi-Sankyo Pharmaceuticals (Y.U.); a Third Term Comprehensive 10-year Strategy for Cancer Control from the Japanese Ministry of Health, Labour and Welfare; and a Grant-in-Aid for Cancer Research from the Ministry of Health, Labour and Welfare of Japan.

References

1 Harper MH, Winter PM, Johnson BH, Eger EI 2nd. Naloxone does not antagonize general anesthesia in the rat. Anesthesiology. 1978;49:3–5.
2 Pace NL, Wong KC. Failure of naloxone and naltrexone to antagonize halothane anesthesia in the dog. Anesth Analg. 1979;58: 36–39.
3 Sarton E, Teppema LJ, Olievier C, Nieuwenhuijs D, Matthes HW, Kieffer BL, et al. The involvement of the mu-opioid receptor in ketamine-induced respiratory depression and antinociception. Anesth Analg. 2001;93:1495–1500.
4 Minami K, Uezono Y. G_q protein-coupled receptors as targets for anesthetics. Curr Pharm Des. 2006;12:1931–1937.
5 Durieux ME. Muscarinic signaling in the central nervous system. Recent developments and anesthetic implications. Anesthesiology. 1996;84:173–189.
6 Minami K, Gereau RW 4th, Minami M, Heinemann SF, Harris RA. Effects of ethanol and anesthetics on type 1 and 5 metabotropic glutamate receptors expressed in *Xenopus* laevis oocytes. Mol Pharmacol. 1998;53:148–156.
7 Minami K, Minami M, Harris RA. Inhibition of 5-hydroxytryptamine type 2A receptor-induced currents by n-alcohols and anesthetics. J Pharmacol Exp Ther. 1997;281:1136–1143.
8 Okamoto T, Minami K, Uezono Y, Ogata J, Shiraishi M, Shigematsu A, et al. The inhibitory effects of ketamine and pentobarbital on substance P receptors expressed in *Xenopus* oocytes. Anesth Analg. 2003;97:104–110.
9 Surratt CK, Adams WR. G protein-coupled receptor structural motifs: relevance to the opioid receptors. Curr Top Med Chem. 2005;5:315–324.
10 Minami K, Uezono Y, Ueta Y. Pharmacological aspects of the effects of tramadol on G-protein coupled receptors. J Pharmacol Sci. 2007;103:253–260.
11 Dascal N. The use of *Xenopus* oocytes for the study of ion channels. CRC Crit Rev Biochem. 1987;22:317–387.
12 Minami K, Uezono Y, Shiraishi M, Okamoto T, Ogata J, Horishita T, et al. Analysis of the effects of halothane on G_i-coupled muscarinic M_2 receptor signaling in *Xenopus* oocytes using a chimeric Gα protein. Pharmacology. 2004;72:205–212.
13 Hojo M, Sudo Y, Ando Y, Minami K, Takada M, Matsubara T, et al. μ-Opioid receptor forms a functional heterodimer with cannabinoid CB_1 receptor: electrophysiological and FRET assay analysis. J Pharmacol Sci. 2008;108:308–319.
14 Vorobiov D, Bera AK, Keren-Raifman T, Barzilai R, Dascal N. Coupling of the muscarinic M_2 receptor to G protein-activated K^+ channels via $G\alpha_z$ and a receptor-$G\alpha_z$ fusion protein. Fusion between the receptor and $G\alpha_z$ eliminates catalytic (collision) coupling. J Biol Chem. 2000;275:4166–4170.
15 Minami K, Vanderah TW, Minami M, Harris RA. Inhibitory effects of anesthetics and ethanol on muscarinic receptors expressed in *Xenopus* oocytes. Eur J Pharmacol. 1997;339:237–244.
16 Dildy-Mayfield JE, Mihic SJ, Liu Y, Deitrich RA, Harris RA. Actions of long chain alcohols on GABAA and glutamate receptors: relation to in vivo effects. Br J Pharmacol. 1996;118:378–384.
17 Jimi N, Segawa K, Minami K, Sata T, SHigematsu A. Inhibitory effects of the intravenous anesthetic, ketamine, on rat mesangial cell proliferation. Anesth Analg. 1997;84:190–195
18 Bohm M, Schmidt U, Gieschik P, Schwinger RH, Bohm S, Erdmann E. Sensitization of adenylate cyclase by halothane in human myocardium and S49 lymphoma wild-type and cyc- cells: evidence for inactivation of the inhibitory G protein $G_i\alpha$. Mol Pharmacol. 1994;45:380–389.
19 Trimer L, Vulliemoz Y, Woo S-Y, Verosky M. Halotane effect on cAMP generation and hydrolysis in rat brain. Eur J Pharmacol. 1980;66:73–80.
20 Maas JW Jr, Vogt SK, Chan GCK, Pineda VV, Storm DR, Muglia LJ. Calcium-stimulated adenylate cyclase are critical modulators of neuronal ethanol sensitivity. J Neurosci. 2005;25:4118–4126.
21 Dascal N. Signalling via the G protein-activated K^+ channels. Cell Signal. 1997;9:551–573.
22 Uezono Y, Akihara M, Kaibara M, Kawano C, Shibuya I, Ueda Y, et al. Activation of inwardly rectifying K^+ channels by GABA-B receptors expressed in *Xenopus* oocytes. Neuroreport. 1998;9: 583–587.
23 Ho BY, Uezono Y, Takada S, Takase I, Izumi F. Coupling of the expressed cannabinoid CB_1 and CB_2 receptors to phospholipase C and G protein-coupled inwardly rectifying K^+ channels. Receptors Channels. 1999;6:363–374.
24 Weigl LG, Schreibmayer W. G protein-gated inwardly rectifying potassium channels are targets for volatile anesthetics. Mol Pharmacol. 2001;60:282–289.
25 Yamakura T, Lewohl JM, Harris RA. Differential effects of general anesthetics on G protein-coupled inwardly rectifying and

other potassium channels. Anesthesiology. 2001;95:144–153.
26 Lewohl JM, Wilson WR, Mayfield RD, Brozowski SJ, Morrisett RA, Harris RA. G-protein-coupled inwardly rectifying potassium channels are targets of alcohol action. Nat Neurosci. 1999;2:1084–1090.
27 Inhibition by ketamine of muscarinic acetylcholine receptor function. Durieux ME. Anesth Analg. 1995;81:57–62.
28 Nagase Y, Kaibara M, Uezono Y, Izumi F, Sumikawa K, Taniyama K. Propofol inhibits muscarinic acetylcholine receptor-mediated signal transduction in *Xenopus* oocytes expressing the rat M_1 receptor. J Pharmacol Sci. 1999;79:319–325.
29 Kovoor A, Celver JP, Wu A, Chavkin C. Agonist induced homologous desensitization of μ-opioid receptors mediated by G protein-coupled receptor kinases is dependent on agonist efficacy. Mol Pharmacol. 1998;54:704–711.
30 Tyrosine phosphorylation of the μ-opioid receptor regulates agonist intrinsic efficacy. Mol Pharmacol. 2001;59:1360–1368.
31 Wieber J, Gugler R, Hengstmann JH, Dengler HJ. Pharmacokinetics of ketamine in man. Anaesthesist. 1975;24:260–263.
32 Idvall J, Ahlgren I, Aronsen KR, Stenberg P. Ketamine infusions: pharmacokinetics and clinical effects. Br J Anaesth. 1979;51:1167–1173.
33 Hirota K, Okawa H, Appadu BL, Grandy DK, Devi LA, Lambert DG. Stereoselective interaction of ketamine with recombinant mu, kappa, and delta opioid receptors expressed in Chinese hamster ovary cells. Anesthesiology. 1999;90:174–182.
34 Kirkpatrick T, Cockshott ID, Douglas EJ, Nimmo WS. Pharmacokinetics of propofol (diprivan) in elderly patients. Br J Anaesth. 1988;60:146–150.
35 Lambert DG, Appadu BL. Muscarinic receptor subtypes: do they have a place in clinical anaesthesia? Br J Anaesth. 1995;74:497–499.
36 Koyama T, Mayahara T, Wakamatsu T, Sora I, Fukuda K. Deletion of μ-opioid receptor in mice does not affect the minimum alveolar concentration of volatile anaesthetics and nitrous oxide-induced analgesia. Br J Anaesth. 2009;103:744–749.
37 Oswald LM, Wand GS. Opioids and alcoholism. Physiol Behav. 2004;81:339–358.
38 Herz A. Endogenous opioid systems and alcohol addiction. Psychopharmacology (Berl). 1997;129:99–111.
39 Vukojevic V, Ming Y, D'Addario C, Rigler R, Johansson B, Terenius L. Ethanol/naltrexone interactions at the mu-opioid receptor. CLSM/FCS study in live cells. PLoS One. 2008;3:e4008.

Neurochemistry International 57 (2010) 923–934

Contents lists available at ScienceDirect

Neurochemistry International

journal homepage: www.elsevier.com/locate/neuint

Activation of the neurokinin-1 receptor in rat spinal astrocytes induces Ca^{2+} release from IP_3-sensitive Ca^{2+} stores and extracellular Ca^{2+} influx through TRPC3

Kanako Miyano [a,b], Norimitsu Morioka [a,*], Tatsuhiko Sugimoto [a], Seiji Shiraishi [b], Yasuhito Uezono [b], Yoshihiro Nakata [a]

[a] Department of Pharmacology, Graduate School of Biomedical Sciences, Hiroshima University, Kasumi 1-2-3, Minami-ku, Hiroshima 734-8551, Japan
[b] Cancer Pathophysiology Division, National Cancer Center Research Institute, 5-1-1, Tsukiji, Chuo-ku, Tokyo 104-0045, Japan

ARTICLE INFO

Article history:
Received 1 July 2010
Received in revised form 9 September 2010
Accepted 20 September 2010
Available online 7 October 2010

Keywords:
Substance P
Spinal astrocyte
Neurokinin-1 receptor
TRPC3 channels
Protein kinase A
Protein kinase C

ABSTRACT

Substance P (SP) plays an important role in pain transmission through the stimulation of the neurokinin (NK) receptors expressed in neurons of the spinal cord, and the subsequent increase in the intracellular Ca^{2+} concentration ($[Ca^{2+}]_i$) as a result of this stimulation. Recent studies suggest that spinal astrocytes also contribute to SP-related pain transmission through the activation of NK receptors. However, the mechanisms involved in the SP-stimulated $[Ca^{2+}]_i$ increase by spinal astrocytes are unclear. We therefore examined whether (and how) the activation of NK receptors evoked increase in $[Ca^{2+}]_i$ in rat cultured spinal astrocytes using a Ca^{2+} imaging assay. Both SP and GR73632 (a selective agonist of the NK1 receptor) induced both transient and sustained increases in $[Ca^{2+}]_i$ in a dose-dependent manner. The SP-induced increase in $[Ca^{2+}]_i$ was significantly attenuated by CP-96345 (an NK1 receptor antagonist). The GR73632-induced increase in $[Ca^{2+}]_i$ was completely inhibited by pretreatment with U73122 (a phospholipase C inhibitor) or xestospongin C (an inositol 1,4,5-triphosphate (IP_3) receptor inhibitor). In the absence of extracellular Ca^{2+}, GR73632 induced only a transient increase in $[Ca^{2+}]_i$. In addition, H89, an inhibitor of protein kinase A (PKA), decreased the GR73632-mediated Ca^{2+} release from intracellular Ca^{2+} stores, while bisindolylmaleimide I, an inhibitor of protein kinase C (PKC), enhanced the GR73632-induced influx of extracellular Ca^{2+}. RT-PCR assays revealed that canonical transient receptor potential (TRPC) 1, 2, 3, 4 and 6 mRNA were expressed in spinal astrocytes. Moreover, BTP2 (a general TRPC channel inhibitor) or Pyr3 (a TRPC3 inhibitor) markedly blocked the GR73632-induced sustained increase in $[Ca^{2+}]_i$. These findings suggest that the stimulation of the NK-1 receptor in spinal astrocytes induces Ca^{2+} release from IP_3-sensitive intracellular Ca^{2+} stores, which is positively modulated by PKA, and subsequent Ca^{2+} influx through TRPC3, which is negatively regulated by PKC.

1. Introduction

Substance P (SP), a member of the tachykinin peptide family, is mainly expressed in primary afferent neurons (Severini et al., 2002). The centrally directed axonal terminals of SP-containing dorsal root ganglion (DRG) neurons project to the superficial lamina of the spinal horn, and their distally directed axonal terminals reside in peripheral tissues. In the spinal dorsal horn, SP released from the central terminals of primary afferent neurons by noxious stimuli activates the SP receptor, neurokinin (NK) receptor, which is expressed on the postsynaptic membrane, thus resulting in the transmission of nociceptive information to the central nervous system (Randic and Miletic, 1977; Hirota et al., 1985).

It is well known that SP binds to all subtypes of NK receptor; NK-1, -2 and -3 (Maggi, 1995). Among the three subtypes, SP has the highest affinity to NK-1 receptor (Maggi and Schwartz, 1997). The stimulation of NK receptors evokes the activation of phospholipase C (PLC), thus leading to phosphoinositol breakdown and an elevation of the intracellular Ca^{2+} concentration ($[Ca^{2+}]_i$) (Maggi, 1995; Snijdelaar et al., 2000). In addition, NK receptors also activate adenylate cyclase in order to induce cyclic AMP production (Nakajima et al., 1992; Maggi, 1995; Snijdelaar et al.,

Abbreviations: 2-APB, 2-aminoethyl diphenylborinate; BIM, bisindolylmaleimide I; BTP2, N-(4-[3,5-bis(trifluoromethyl)-1H-pyrazol-1-yl]phenyl)-4methyl-1,2,3-thiadiazole-5-carboxamide; $[Ca^{2+}]_i$, intracellular Ca^{2+} concentration; DAG, diacylglycerol; DMEM, Dulbecco's modified Eagle's medium; DRG, dorsal root ganglion; fura-2 AM, fura-2 acetoxymethyl ester; GFAP, glial fibrillary acidic protein; Hank's buffer, Hanks' balanced salt solution; IP_3, inositol 1,4,5-triphosphate; NK, neurokinin; PLC, phospholipase C; PKA, protein kinase A; PKC, protein kinase C; Pyr3, ethyl-1-(4-(2,3,3-trichloroacrylamide)phenyl)-5-(trifluoromethyl)-1H-pyrazole-4-carboxylate; SP, substance P; TRPC channel, canonical transient receptor potential channel.

* Corresponding author. Tel.: +81 82 257 5312; fax: +81 82 257 5314.
E-mail addresses: mnori@hiroshima-u.ac.jp, mnori@hiroshima-u.ac (N. Morioka).

0197-0186/$ – see front matter © 2010 Elsevier Ltd. All rights reserved.
doi:10.1016/j.neuint.2010.09.012

2000). Recent studies have shown that spinal astrocytes, the major population of glia supporting neurons, also express functional NK-1 receptor (Marriott et al., 1991; Palma et al., 1997). Therefore, SP released from the nerve terminal may act not only neurons, but also on the astrocytes surrounding synaptic junctions in the spinal cord. In this manner, SP may induce the increase of $[Ca^{2+}]_i$ via spinal astrocytes. This successive event has an important role in communication between neurons and astrocytes, and might be essential to achieve the synaptic transmission (Fields and Stevens-Graham, 2002). It is therefore possible that NK receptors on spinal astrocytes may also be associated with SP-related pain transmission. Although it has been showed that the activation of the NK-1 receptor on spinal astrocytes produces inositol 1,4,5-tripsophate (IP_3) (Marriott et al., 1991; Palma et al., 1997), the Ca^{2+} signaling induced by the activation of that receptor in spinal astrocytes has not yet been investigated.

Recently, activation of the PLC-linked receptor (histamine receptor and proteinase-activated receptor) was reported to induce Ca^{2+} release from the intracellular Ca^{2+} stores through the IP_3 receptor, and also has been shown to cause the influx of extracellular Ca^{2+} in human astrocytoma (Barajas et al., 2008; Nakao et al., 2008). Several reports have demonstrated that the family of canonical transient receptor potential (TRPC) channels is one of candidate receptors responsible for mediating the extracellular Ca^{2+} influx induced after the activation of PLC-linked receptors in vasucular smooth muscle and TRPC channel-expressing cells (Venkatachalam and Montell, 2007; Large et al., 2009). Moreover, functional TRPC channels are also expressed in human astrocytoma (Barajas et al., 2008; Nakao et al., 2008). Therefore, these reports indicate the possibility that the NK-1 receptor-stimulated increase in $[Ca^{2+}]_i$ by spinal astrocytes involves the Ca^{2+} influx through TRPC channels. However, it is unclear whether the stimulation of the NK-1 receptor causes Ca^{2+} influx though TRPC channels in spinal astrocytes. The present study is the first to demonstrate that the activation of the NK-1 receptor by SP or GR73632, a selective NK-1 receptor agonist, evoked an increase in $[Ca^{2+}]_i$ in cultured spinal astrocytes, which involved both Ca^{2+} release from intracellular Ca^{2+} stores, and extracellular Ca^{2+} influx through the TRPC channels.

2. Materials and methods

2.1. Materials

The following drugs and reagents were used for the present studies: bisindolylmaleimide I (BIM) and N-(4-[3,5-bis(trifluoromethyl)-1H-pyrazol-1-yl]phenyl)-4methyl-1,2,3-thiadiazole-5-carboxamide (BTP2) (Calbiochem, La Jolla, CA, USA); Fetal calf serum (Biological Industries, Kibbutz Beit Haemek, Israel); fura-2 acetoxymethyl ester (fura-2 AM) (Dojindo Laboratories, Kumamoto, Japan); 2.5% trypsin (Gibco-BRL, Gaithersburg, MD, USA); Dulbecco's modified Eagle's medium (DMEM) (Nissui, Tokyo, Japan); 2-aminoethyl diphenylborinate (2-APB), GR94800, H89, Hanks' balanced salt solution (Hanks' buffer), penicillin/streptomycin, poly-L-lysine, SB222200, thapsigargin, U73122 and xestospongin C (Sigma Chemical, St. Louis, MO, USA); SP (Peptide Institute, Osaka, Japan); CP96345 (Pfizer Central Research, Groton, CT, USA); DNase (Roche, Basel, Switzerland). Ethyl-1-(4-(2,3,3-trichloroacrylamide)phenyl)-5-(trifluoromethyl)-1H-pyrazole-4-carboxylate (Pyr3) was kindly provided by Prof. Y. Mori of Kyoto University (Japan). All other reagents were of the highest purity available from commercial sources.

2.2. Cell culture

Spinal astrocytes were prepared from spinal cords of neonatal Wistar rats according to a previously reported method (Morioka et al., 2009). In brief, the isolated spinal cords were minced, and then incubated with trypsin and DNase. Dissociated cells were suspended in DMEM supplemented with 10% fetal calf serum and penicillin/streptomycin (100 U/ml and 100 μg/ml, respectively). Thereafter, cell suspensions were plated in 75 cm^2 tissue culture flasks (7.5 to 10×10^6 cells/flask) precoated with poly-L-lysine (10 μg/ml). The cells were maintained in a 10% CO_2 incubator at 37 °C. After 10 days, microglial cells were removed by vigorously shaking the growth flasks. Thereafter, the cells were harvested and replated to 35 mm diameter dishes at a density of 3×10^5 cells/dish, or glass coverslips with a silicon rubber wall (FlexiPERM; Heraeus Biotechnology, Hanau, Germany) at a density of 0.2×10^5 cells/slide. At 3 days post-seeding, the medium was replaced with serum-free DMEM. The cells were used for experiments overnight after the medium change. Prepared astrocytes showed a purity >95% as determined by glial fibrillary acidic protein (GFAP) immunoreactivity. All animal procedures were performed in accordance with the Guide for Animal Experimentation, Hiroshima University and the Committee of Research Facilities for Laboratory Animal Sciences, Graduate School of Biomedical Sciences, Hiroshima University, Japan.

2.3. Measurement of $[Ca^{2+}]_i$ in spinal astrocytes

The measurement of $[Ca^{2+}]_i$ was performed using a previously described method (Miyano et al., 2009). All experiments were performed in Ca^{2+} (1.3 mM)-containing or Ca^{2+}-free Hanks' buffer. Spinal astrocytes were loaded with 5 μM of fura-2 AM in Ca^{2+}-containing Hanks' buffer for 50 min at 37 °C. After washing, the cells treated with either SP or GR73632 in Ca^{2+}-containing or Ca^{2+}-free Hanks' buffer, respectively. The fluorescence intensity was measured with the excitation wavelengths of 340 and 380 nm and the emission wavelength of 510 nm. The video image output was digitized by an Argus Hisca color image processor (Hamamatsu Photonics, Shizuoka, Japan).

2.4. RT-PCR analysis

According to a previously reported method (Morioka et al., 2009), total RNA in astrocytes was prepared and used to synthesize cDNA with MuLV reverse transcriptase (Applied Biosystems, Foster City, CA) and a random hexamer primer (Takara Bio Inc., Shiga, Japan). PCR reactions were performed with the specific primers indicated in Table 1 and AmpliTaq Gold™ (Applied Biosystems) at 95 °C for 10 min followed by 35–40 cycles (Table 1) of denaturation at 95 °C for 30 s, annealing at 57 °C for 30 s, and elongation at 72 °C for 2 min, with a final extension at 72 °C for 5 min. The resulting PCR products were analyzed on a 1.5% agarose gel and had the size expected from the known cDNA sequence.

2.5. Immunofluorescence staining

Cells were washed with PBS(−), fixed with 4% paraformaldehyde, and permeabilized with 0.1% triton-X at room temperature. After blocking with 3% BSA, cells were incubated with a polyclonal antibody against the NK-1 receptor (1:100; Sigma), TRPC3 (1:100; AnaSpec Inc., San Jose, CA), or a monoclonal antibody against GFAP (1:200; Sigma) for 1 h at room temperature. Next, the cells were further incubated with Alexa 546-conjugated anti-rabbit IgG antibody, or Alexa 488-conjugated anti-mouse IgG antibody (1:500, Molecular Probes, Invitrogen, Carlsbad, CA) for 1 hour at room temperature. Immunolabeled cells were visualized under a Zeiss LSM510 META confocal microscope (Carl Zeiss, Jene, Germany).

2.6. Statistical analysis

The data are presented as the means ± S.E.M. of at least three independent experiments. The statistical analysis of all data except for Fig. 3F, was performed by a one-way analysis of variance (ANOVA) followed by Bonferroni's test. In Fig. 3F, *t*-test was used to analyze the differences between the two groups. A probability value (p) of less than 0.05 was considered to be statistically significant.

Table 1
The primer sequences and sizes of PCR products of rat TRPC channels.

Subtypes of TRPC	Forward primers (5′→3′)	Reverse primers (3′→5′)	Size (bp)
C1	TCTGGCCAGTCCAGCTCTAA	CCCTTCATACCACAGCCTCT	682
C2	CCCTGCAACCATGCTCATGT	CTTGAGCTGGACAACGGTCT	609
C3	CTTGATCCAGGCTGGGGAAA	CTTTGGCCCCAAGGTAGTAG	708
C4	CTCGCTCATTGCGCTGTCAA	GTCGATGTGCTGAGAGGCTA	547
C5	GCCAAGCTGAAGGTGGCAAT	AGATCTGCAGAGGCCCTAAG	664
C6	GACTCCTTCAGCCACTCTAG	ACGAGCAGCCCCAGGAAAAT	561
C7	TCCCTTTAACCTGGTGCCGA	TCACCCTCAGGTGGTCTTTG	449

3. Results

3.1. Increase in $[Ca^{2+}]_i$ by spinal astrocytes through NK-1 receptor activation

In the presence of extracellular Ca^{2+}, SP evoked an increase in the $[Ca^{2+}]_i$ in a dose-dependent manner at a concentration range of 1–100 nM as shown in Fig. 1A–C. The Ca^{2+} response rapidly peaked after treatment with SP, and then gradually returned toward the basal level within several minutes. The extent of the SP-induced increase in $[Ca^{2+}]_i$ was calculated using the differences between the fura-2 fluorescence ratio (340/380) of the resting level observed before SP treatment and the peak level obtained after SP treatment (Fig. 1G). Next, we investigated which subtypes of NK receptors were involved in the increase of $[Ca^{2+}]_i$ in cells treated with 100 nM of SP. The SP-induced increase in $[Ca^{2+}]_i$ was completely suppressed by pretreatment with CP-96346 (10 μM), a selective antagonist of the NK-1 receptor (Fig. 1D and H). In contrast, neither GR94800 (10 μM), a selective NK-2 antagonist, nor SB222200 (10 μM), a selective NK3 antagonist, affected the SP-

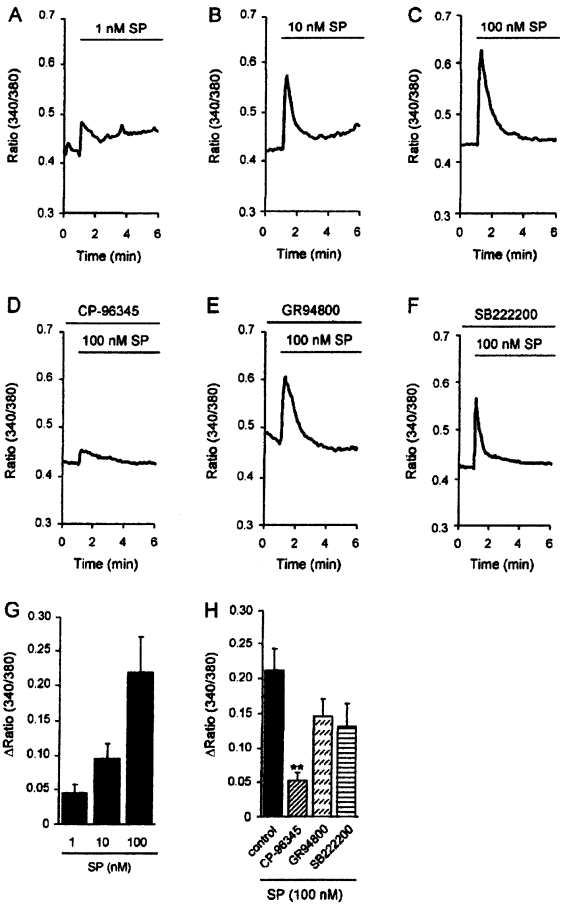

Fig. 1. Mobilization of $[Ca^{2+}]_i$ in spinal astrocytes stimulated with SP. The trace in each graph (A–F) shows the representative mean $[Ca^{2+}]_i$ in randomly selected cells. The fura 2-loaded cells were treated with 1–100 nM of SP in Hanks' buffer, respectively (A–C). After the cells were pretreated with 10 μM of CP96345 (D), GR94800 (E) or SB222200 (F) for 20 min, then cells were stimulated with 100 nM of SP. The extent of the increase in $[Ca^{2+}]_i$ induced by SP was quantified by determining the differences between the ratio (340/380) of the basal and the peak level obtained after SP treatment (G and H). The data are expressed as the means ± S.E.M. (*bars*) of separate experiments. $^{**}p < 0.01$ in comparison with the value for the cells treated with SP alone.

mediated increase in $[Ca^{2+}]_i$ (Fig. 1E, F and H). Moreover, we showed the co-localization of the NK-1 receptor and GFAP, which is a defined marker for astrocytes, by immunofluorescence staining (Fig. 2). In addition, it was indicated that the NK-1 receptor is mostly expressed in the plasma membrane of spinal astrocytes. Taken together, these data suggest that SP induces the increase in $[Ca^{2+}]_i$ in spinal astrocytes through stimulation of the NK-1 receptor.

In addition, we examined the effect of GR73632, a selective agonist of the NK-1 receptor, on the increase in $[Ca^{2+}]_i$. As shown in Fig. 3A–C and E, treatment with GR73632 at a concentration range of 10–1000 nM evoked a transient and sustained increase in $[Ca^{2+}]_i$ in a dose-dependent manner. The Ca^{2+} response activated by GR73632 was similar to that following SP exposure. In addition, preincubation with CP-96346 specifically blocked the GR73632-induced increase of $[Ca^{2+}]_i$ (Fig. 3D and F). As these data suggest that the NK-1 receptor contributes to the mobilization of $[Ca^{2+}]_i$, GR73632 was used for further investigation of the NK-1 receptor-mediated increase in $[Ca^{2+}]_i$ by spinal astrocytes.

3.2. Regulation of both Ca^{2+} release from Ca^{2+} stores and the influx of extracellular Ca^{2+} in spinal astrocytes by activation of the NK-1 receptor

As the regulation of $[Ca^{2+}]_i$ is associated with both the release of Ca^{2+} from intracellular Ca^{2+} stores and the influx of extracellular Ca^{2+}, the involvement of both of these processes in the GR73632-induced increase in $[Ca^{2+}]_i$, was examined by stimulating spinal astrocytes with 1000 nM GR73632 in Hanks' buffer with or without Ca^{2+}. In the presence of extracellular Ca^{2+} (1.3 mM), GR73632 induced both a transient and sustained increase of $[Ca^{2+}]_i$ as shown in Fig. 4A. On the other hand, in the absence of extracellular Ca^{2+}, only a transient increase in $[Ca^{2+}]_i$, which rapidly peaked and returned toward the basal level within 2 min after $[Ca^{2+}]_i$ reached to a peak, was observed after treatment with GR73632 (Fig. 4B). In addition, the increase in $[Ca^{2+}]_i$ induced by GR73632 was completely attenuated in the Ca^{2+}-free Hanks' buffer by preincubation with thapsigargin (1 μM), which depletes Ca^{2+} in intracellular Ca^{2+} stores by inhibiting Ca^{2+}-ATPase (Fig. 4C). Taken together, these data suggest that GR73632 induces both Ca^{2+} release from Ca^{2+} stores and also Ca^{2+} influx. Therefore, we defined the change in $[Ca^{2+}]_i$ at the transient peak to be the result of the Ca^{2+} release from Ca^{2+} stores (Fig. 4D). On the other hand, the change in $[Ca^{2+}]_i$ (compared to baseline) 2 min after the peak $[Ca^{2+}]_i$ was defined as the extent of Ca^{2+} influx (Fig. 4E).

3.3. Influence of intracellular signaling molecules on the GR73632-induced increase of $[Ca^{2+}]_i$ by spinal astrocytes

It is well known that stimulation of the NK-1 receptor activates PLC, which produces both inositol 1,4,5-triphosphate (IP_3) and diacylglycerol (DAG) by the breakdown of phosphatidylinositol

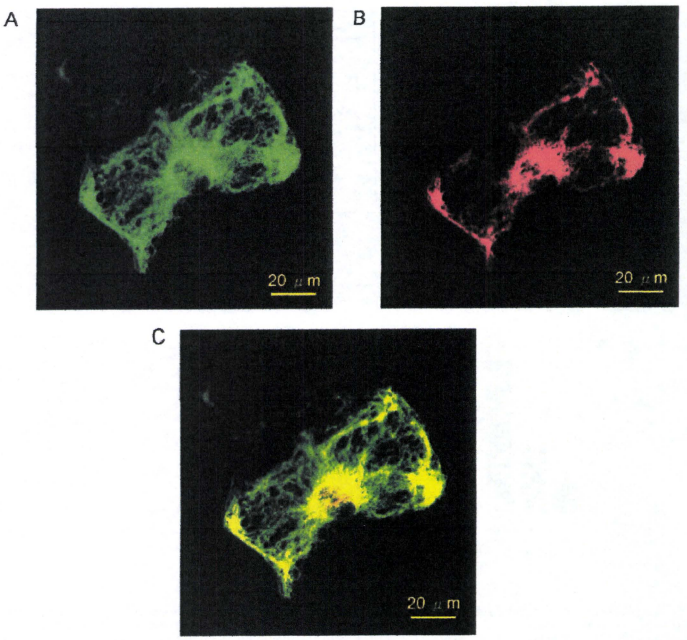

Fig. 2. Spinal astrocytes express the NK-1 receptor. Immunofluorescent analysis of GFAP (green; A) and the NK-1 receptor (red; B) expression in cultured spinal astrocytes. The expression of the NK-1 receptor was found in GFAP-labeled cells (C).

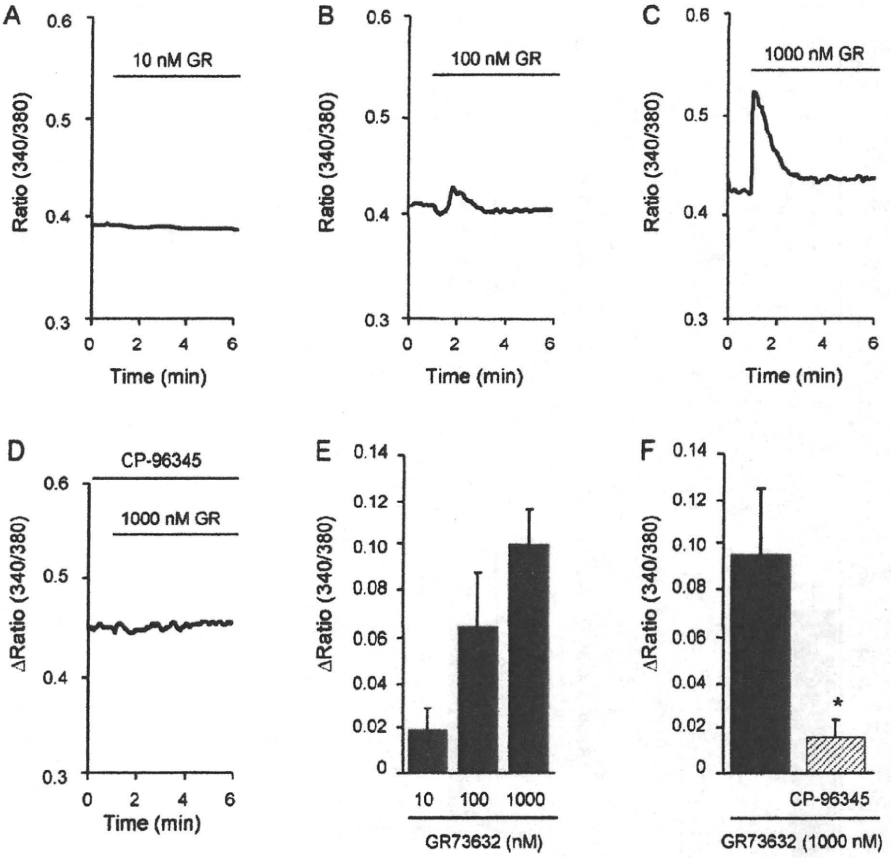

Fig. 3. Mobilization of $[Ca^{2+}]_i$ in spinal astrocytes stimulated with GR73632. The trace in each graph (A–D) shows the representative mean $[Ca^{2+}]_i$ in randomly selected cells. The fura-2-loaded cells were treated with 10–1000 nM of GR73632 (GR) in Hanks' buffer (A–C). After the cells were pretreated with 10 μM of CP96345 (D) for 20 min, then cells were stimulated with 1000 nM of GR73632. The extent of the increase in $[Ca^{2+}]_i$ induced by GR73632 was quantified by determining the differences between the ratio (340/380) of the basal and the peak level obtained after GR73632 treatment (E and F). The data are expressed as the means ± S.E.M. (*bars*) of separate experiments. $^*p < 0.05$ in comparison with the value for the cells treated with GR73632 alone.

4,5-bisphosphates. Therefore, we investigated the involvement of PLC and/or the IP_3 receptor in the increase of $[Ca^{2+}]_i$ following treatment with 1000 nM of GR73632. Pretreatment with U73122 (10 μM), a PLC inhibitor, or xestospongin C (1 μM), an inihibitor of the IP_3 receptor, completely inhibited the GR73632-induced increase in $[Ca^{2+}]_i$ (Fig. 5A–C). In addition, 2-APB, which inhibits both the IP_3 receptor and the subsequent Ca^{2+} influx (Zhou et al., 2007), also significantly suppressed the action of GR73632 (Fig. 5D). Quantitative data showed that all of these inhibitors blocked both Ca^{2+} release from intracellular Ca^{2+} stores and extracellular Ca^{2+} influx caused by GR73632 (Fig. 5G and H). These data suggest that the GR73632-mediated increase in $[Ca^{2+}]_i$ involves the activation of PLC and the IP_3 receptor.

Since activation of the NK-1 receptor is likely to be coupled to both Gq- and Gs-proteins (Holst et al., 2001), PKA may also be activated by stimulation of the NK-1 receptor. Therefore, we compared the influence of inhibitors of either PKA or PKC on the GR73632-induced increase in $[Ca^{2+}]_i$. Preincubation with H89 (10 μM), a PKA inhibitor, attenuated the GR73632-mediated increase in $[Ca^{2+}]_i$ (Fig. 5F). In contrast, pretreatment with BIM (10 μM), a PKC inhibitor, significantly enhanced the effect of GR73632 (Fig. 5E). Quantitative analysis data indicated that H89 significantly blocked the GR73632-induced Ca^{2+} release from intracellular Ca^{2+} stores, but did not affect the influx of extracellular Ca^{2+} (Fig. 5G and H). On the other hand, BIM (10 μM) markedly enhanced the GR73632-mediated Ca^{2+} influx without affecting the Ca^{2+} release from intracellular stores (Fig. 5G and H).

To further elucidate the involvement of these intracellular signaling molecules in the GR73632-mediated increase in $[Ca^{2+}]_i$, we investigated the effects of 2-APB, H89 or BIM on the GR73632-induced changes in $[Ca^{2+}]_i$ under Ca^{2+} free conditions, and following the addition of Ca^{2+} in the buffer. As shown in Fig. 6B, after a rapid and transient increase in $[Ca^{2+}]_i$ induced by GR73632 in Ca^{2+}-free Hanks' buffer, the addition of $CaCl_2$ led to a sustained increase in $[Ca^{2+}]_i$, indicating that this response was due to the influx of extracellular Ca^{2+}. Pretreatment with 2-APB inhibited both components (release from stores and extracellular influx) evoked by GR73632 treatment (Fig. 6C, F and G). H89 significantly suppressed only the release of Ca^{2+} from intracellular stores (Fig. 6E–G). In contrast, pretreatment with BIM enhanced only the GR73632-induced Ca^{2+} influx, but not Ca^{2+} release (Fig. 6D, F and G). Taken together, these data suggest that PKA regulates the GR73632-induced Ca^{2+} release from intracellular Ca^{2+} stores, whereas PKC has a negative impact on the GR73632-induced influx of extracellular Ca^{2+}.

3.4. Involvement of TRPC channels in the GR73632-induced increase in $[Ca^{2+}]_i$ by spinal astrocytes

TRPC, non-selective cation channels, are classified into TRPC1–7 (Venkatachakam and Montell, 2007). As we found that TRPC1, 3, 4, 5, and 6 channels were expressed on spinal astrocytes using RT-PCR (Fig. 7A), we examined which subtypes of TRPC channel are involved in the GR73632-induced increase in $[Ca^{2+}]_i$ by using TRPC channel inhibitors. Either BTP2 (10 μM), a general blocker of TRPC